

# TOWARDS 100% POLARIZATION IN THE OPTICALLY-PUMPED POLARIZED ION SOURCE\*

A. Zelenski, J. Alessi, A. Kponou, J. Ritter, V. Zubets  
 Brookhaven National Laboratory, Upton, NY 11973, U.S.A.

**Abstract.**

The depolarization factors in the multi-step spin-transfer polarization technique and basic limitations on maximum polarization in the OPPIS (Optically-Pumped Polarized H Ion Source) are discussed. Detailed studies of polarization losses in the RHIC OPPIS and the source parameters optimization resulted in the OPPIS polarization increase to 86-90%. This contributed to increasing polarization in the AGS and RHIC to 65 ~ 70%.

## INTRODUCTION

In the BNL Optically Pumped Polarized H Ion Source, an ECR-type source produces a primary proton beam of 2.8 ~ 3.0 keV energy, which is converted to electron-spin polarized H atoms by electron pick-up in an optically pumped Rb vapor cell. Electrostatic deflection plates downstream of the polarized alkali remove any surviving H<sup>+</sup> or other charged species. The electron-polarized H beam then passes through a magnetic field reversal region, where the polarization is transferred to the nucleus, via hyperfine interaction (Sona transition). The polarized H atoms are then negatively ionized in a Na-jet vapor cell to form nuclear polarized H-ions (see Fig. 1). Alternatively, the H atoms can be ionized in a He gaseous cell to form polarized protons. This source is capable of producing in excess of 1.6 mA polarized H<sup>-</sup> ion current in dc operation /1/.

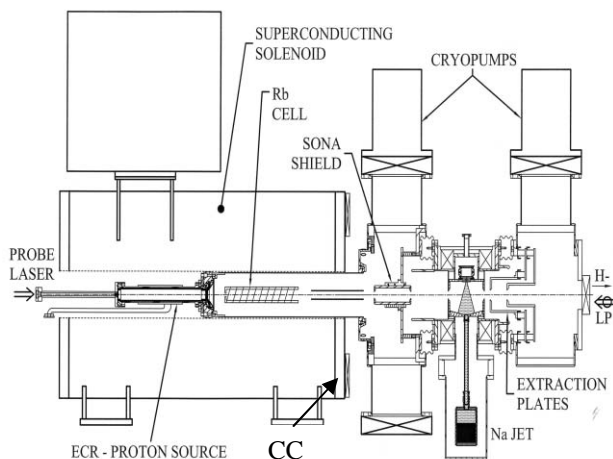


Fig.1. The general layout of the BNL OPPIS.

The OPPIS technique is a multi-step polarization-transfer process. In the first step, electron spin polarized atoms are produced, in the second step, the electron polarization is transferred to the nuclei by means of the hyperfine interaction, and in the last step, nuclear spin

polarized atoms are ionized. At each step there is some loss of polarization, which can be expressed as follows:

$$P = P_{Rb} \cdot S \cdot B_{H2} \cdot E_{LS} \cdot E_{Sona} \cdot E_{ion} \cdot M \cdot X,$$

where  $P_{Rb}$  is an average Rb vapor polarization,  $S$  represents the degree of matching between the Rb polarization profile and the spatial proton beam profile,  $B_{H2}$  is a factor accounting for proton neutralization by residual hydrogen from the ECR source,  $E_{LS}$  accounts for spin-orbital depolarization of hydrogen atoms (produced in excited states),  $E_{Sona}$  is the efficiency of the Sona transition,  $E_{ion}$  is a polarization loss in the ionization process,  $M$  accounts for polarization dilution by molecular H<sub>2</sub><sup>+</sup> ions produced in the ECR source, and  $X$  represents other factors (for example polarization loss between source and 200 MeV polarimeter). The detailed studies and optimization of each of these factors resulted in 86% polarization in Run 2006, and further increase to 88~90% in Run 2007. The polarization loss factors were discussed in earlier papers /2,3/. Here we report the reduction of losses in the  $B_{H2}$ ,  $E_{Sona}$  and  $E_{ion}$  factors.

**Proton neutralization in the residual hydrogen gas from the ECR source –  $B_{H2}$ .** The neutralization of the primary proton beam from the ECR source in residual hydrogen gas upstream of and inside the Rb cell, produces unpolarized hydrogen atoms, which dilute polarization. The factor  $B_{H2}$  can be calculated from polarization and current measurements at low Rb vapor thickness. It depends on the extraction grid and Rb cell geometry, and vacuum chamber conductance and pumping speed. Some neutralization occurs on the atomic and molecular hydrogen gas flowing along the Rb cell axis and can be reduced only by increasing the proton/neutral fraction ratio out of the ECR source. The recent optimization of the Rb cell and vacuum chamber geometry (the cell length was reduced from 30 cm to 20 cm and moved further downstream from the ECR source, and the cell support and cooling screen were redesigned to improve vacuum conductance) significantly reduced hydrogen flow inside the Rb cell. This resulted in significant polarization gain at low Rb thicknesses (see Fig. 2).

**Sona-transition efficiency -  $E_{Sona}$ .** The electron polarization is transferred to protons by the Sona-transition technique as the electron-spin polarized atomic H beam passes through a magnetic field reversal region in between high field “polarizer” solenoid and ionizer solenoid. Very strict restrictions are applied to the transverse magnetic field in the zero-crossing region (where the longitudinal field reverses direction) to avoid spin-flip /4/. The longitudinal field gradient generates a transverse field  $\mathbf{B}_r$ :  $\mathbf{B}_r = \mathbf{r}/2(d\mathbf{B}/dz)$ , and to fulfill Sona-

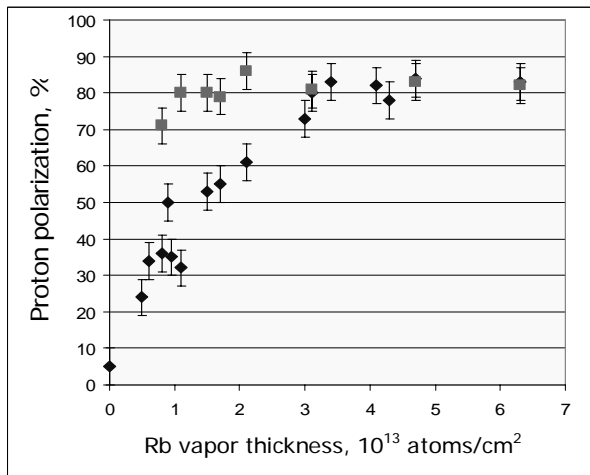


Fig. 2. Proton polarization at 200 MeV vs. Rb vapor thickness before ( $\blacklozenge$ ) and after ( $\blacksquare$ ) the Rb cell upgrade.

transition conditions (for a 2 cm  $\varnothing$  atomic hydrogen beam) the  $d\mathbf{B}/dz \ll 0.2$  G/cm is required at the  $\mathbf{B}z=0$  crossing point. A “soft” steel cylindrical Sona-shield and Correction Coil (CC) were designed and built to reduce the field gradient to less than 0.2 G/cm in the limited space between superconducting solenoid 25 kG field and ionizer solenoid 1.5 kG field. As a result of Sona-shield and correction coil optimization, the gradient was reduced to less than 0.09 G/cm (see Fig. 3, magnetic field calculations, which were confirmed by field measurements).

For the Sona-transition, efficiency studies and optimization the polarization dependence vs. correction coil current was measured in a wide range of CC field. Polarization was measured in the Lamb-shift polarimeter at 35 keV beam energy and at 200 MeV in the p-Carbon polarimeter. Typical results are presented in Fig. 4. Since the CC field direction is opposite to superconducting solenoid field, the zero-crossing point is moving inside the Sona-shield upstream, when CC current is increased. This reduces the gradient and slightly increases polarization. At some current value the zero-crossing point is pushed out of the shield and the gradient is greatly increased (see Fig.3), which causes a steep polarization drop. This is an expected result and it was observed in previous experiments at the TRIUMF OPPIS [2] and initial tests at the RHIC OPPIS. A new, stronger, correction coil (and additional magnetic shield at the superconducting solenoid flange) allowed significant expansion of the field variation range, which revealed unexpected periodic polarization quantum oscillations. The polarization almost completely recovered at higher CC field, and the oscillations have a period of about 5 A correction coil current increment. The amplitude of the oscillations is slowly decreased with higher CC field. To further explore this effect, the CC field was reversed. This pushed the zero-crossing upstream outside of the shield, and the polarization oscillations were also observed. The field gradients at zero-crossing region were calculated. The resonance-like polarization oscillations are going through maximum with an increment of about 5 G/cm.

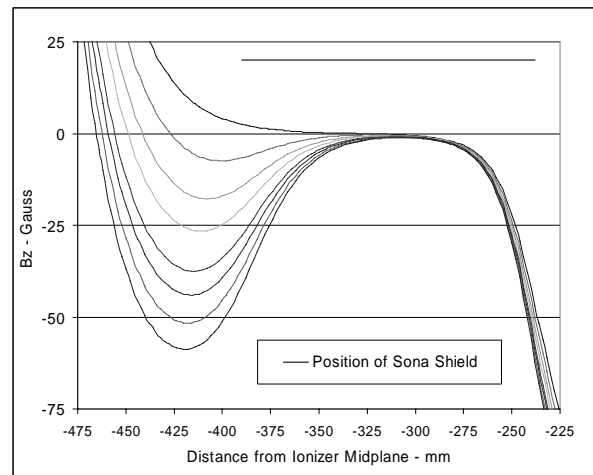


Fig. 3. Calculated magnetic field profiles in the Sona transition region for several correction coil currents corresponding to polarization oscillation peaks.

An atom passing the field reversal region at 1 cm off axis will “see” about 2.5 G transverse magnetic field. The Larmor electron spin precession in this field will be:  $\omega \cdot B \cdot t = 2\pi \cdot 28 \cdot 10^9$  B·t. The precession time  $t$  is the atom travel time through zero-crossing region of about 5 cm long, which for 3.0 keV atoms (at speed  $7 \cdot 10^7$  cm/s) is equal to:  $t \sim 1.4 \cdot 10^{-7}$  s. This gives:  $\omega \cdot B \cdot t \approx 2\pi$ , which gives rise to the double spin flip in between polarization maximums and single spin flip when polarization drops to minimum. This transverse field induces the spin-flip for only one of two electron spin polarized atomic hydrogen state:  $\langle 1 \rangle = (m_j=1/2, m_l=1/2)$ . The other, “mixed”, state:  $\langle 2 \rangle = [(m_j=1/2, m_l=-1/2) + (m_j=1/2, m_l=1/2)]$  - adiabatically follows the reversing field direction.

Also the radial field distribution and spin flip conditions are different for atoms at different radii. This affects the amplitude of polarization oscillations, which can vary between 15~50 % for different Sona transition configurations. The stronger radial dependence at higher field gradients reduces the coherency of spin flip, which decreases both the polarization and the oscillation amplitude (see Fig. 4).

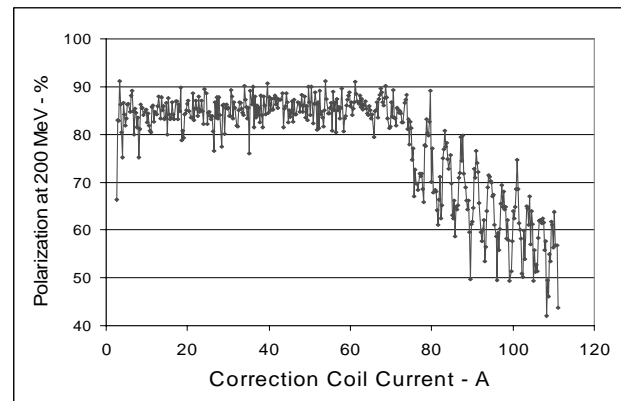


Fig. 4.  $H^-$  Polarization measured at the 200 MeV polarimeter. Sona-shield collimator diameter – 2.0 cm, ionizer solenoid field 1.9 kG.

The minimal field gradient and maximum polarization is obtained just before the field dip, providing that all the other transverse field sources are eliminated by the Sona shield (an additional  $\mu$ -metal shield layer was inserted inside the “soft” steel cylinder to suppress the small residual field of the steel itself). The polarizations for different beam diameters – 1.2 cm, 1.6 cm and 2.0 cm (beam diameter is defined by the collimator at the entrance of Sona-shield) were measured after this optimization and, within errors, the maximum polarization values are the same. This means that Sona-transition efficiency is close to 100% (the best value for further estimations is:  $E_{\text{Sona}} = 0.99 \pm 0.01$ ).

**Polarization loss in Na-jet ionizer cell –  $E_{\text{ion}}$ .** To break the electron-proton hyperfine interaction, a magnetic field of about 1.5 kG is required in the sodium-jet ionizer cell. Since the critical field for hydrogen atoms is 507.6 G, the theoretical polarization loss at this field is  $\sim 3\%$ , and increasing the ionizer field over 1.5 kG is not very effective for improving the polarization (the theoretical increase in polarization at 1.5 kG and 2.0 kG is only  $\sim 1\%$ ); but it will cause beam emittance growth beyond the RFQ acceptance and result in beam intensity losses.

Significantly higher polarization growth at higher ionizer fields was observed in experiments (see Fig.5). This means that there is another effect, which also depends on the ionizer field strength. One possible explanation might be an observed polarization dependence on the Na-jet vapor thickness. Usually the jet cell is operated at sodium reservoir temperature of  $\sim 500^\circ\text{C}$ , which is required for the H<sup>+</sup> ion yield saturation (the estimated total jet thickness is  $\sim 2 \cdot 10^{15}$  atoms/cm<sup>2</sup>). At  $470^\circ\text{C}$  temperature, jet thickness is reduced to  $\sim 1.0 \cdot 10^{15}$  atoms/cm<sup>2</sup>, the H<sup>+</sup> current drops to about 80% of maximum, and the polarization is increased by  $\sim 2\text{-}3\%$ . The stronger ionizer field would suppress this depolarization process and increase polarization beyond hyperfine interaction breaking limit.

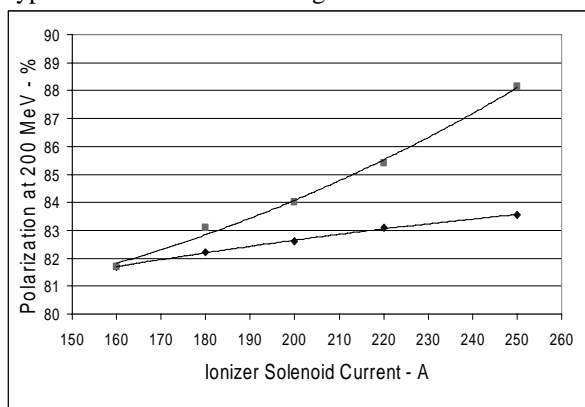


Fig.5. Measured (■) and calculated (◆) polarization vs. ionizer solenoid field strength. Ionizer field at 250 A current is equal to 1.98 kG.

The factor  $E_{\text{ion}}$  is presently estimated at:  $E_{\text{ion}} \sim 0.97\text{-}0.98$  (for ionizer field of 1.5–2.0 kG). The benefit of the higher ionizer field for increasing polarization is partially offset by current reduction due to emittance growth, which is

proportional  $\sim BR^2$ . This limits the beam radii to less than  $\sim 0.8$  cm, and ionizer magnetic field to less than 2.0 kG. A higher brightness polarized atomic H beam is required to keep beam emittance in the RFQ acceptance range at high field by using smaller diameter collimated beam.

## OPPIS WITH THE “FAST ATOMIC HYDROGEN BEAM SOURCE”

In pulsed operation suitable for application at high-energy accelerators and colliders, the ECR source limitations can be overcome by using instead a high brightness proton source outside the magnetic field /6/. Following neutralization in hydrogen, the high brightness 3.0–4.0 keV atomic H beam is injected into a superconducting solenoid, where both a He ionizer cell and an optically-pumped Rb cell are situated in the same 25–30 kG solenoidal field, required to preserve the electron-spin polarization. The injected H atoms are ionized in the He cell with 80% efficiency to form a low emittance intense proton beam, which enters the polarized Rb vapor cell. The protons pick up polarized electrons from the Rb atoms to become a beam of electron-spin polarized H atoms. A negative bias of about 1.0 kV applied to the He cell decelerates the proton beam produced in the cell. This allows energy separation of the polarized hydrogen atoms produced in Rb vapor cell and hydrogen atoms of the primary beam.

Atomic hydrogen beam current densities greater than 100 mA/cm<sup>2</sup> can be obtained at the Na jet ionizer location (about 180 cm from the source) by using a very high brightness fast atomic beam source developed at BINP, Novosibirsk /7/, and tested in experiments at TRIUMF/1/, where more than 10 mA polarized H<sup>+</sup> and 50 mA proton beam intensity was demonstrated /1/.

Higher polarization is also expected with the fast atomic beam source due to: a) elimination of neutralization in residual hydrogen -  $B_{\text{H}_2} \sim 1$ ; b) better Sona-transition efficiency for the smaller  $\sim 1.5$  cm diameter beam; c) use of higher ionizer field (up to 3.0 kG), while still keeping the beam emittance below  $2.0 \pi$  mm·mrad, because of the smaller,  $\sim 1.5$  cm, beam diameter.

All these factors combined will further increase polarization in the pulsed OPPIS to over 90% and the source intensity to over 10 mA. The ECR-source replacement with an atomic hydrogen injector will provide the high intensity beam for polarized RHIC luminosity upgrade and for future eRHIC facilities.

The authors are thankful to Prof. T. Clegg, UNC and TUNL, for very helpful discussions on Sona transition features and the observed polarization oscillations.

## REFERENCES

- [1] A. Zelenski, Proc.SPIN2000, **AIP 570**, p.179, (2000).
- [2] A. Zelenski et al., **NIM A334**, p.285, (1993).
- [3] A. Zelenski et al., SPIN2002, **AIP 675**, p.881, (2003).
- [5] P. G. Sona, *Energia Nucl.*, **14**, p.295, (1967).
- [6] A. Zelenski et al., **NIM A245**, p.223, (1986).
- [7] V. Davydenko, **NIM A427**, p.230, (1999).